Modern sea surface productivity and temperature estimations off Chile as detected by coccolith accumulation rates

Saavedra-Pellitero, M. (1), Baumann, K-H. (1), Hernández-Almeida, I. (2), Flores, J.A. (3), and Sierro, F.J. (3)

(1) University of Bremen, Department of Geosciences, Klagenfurter Strasse, 28359, Bremen (Germany)

(2) University of Bern, Institute of Geography, Erlachstrasse 9a, CH-3012, Bern (Switzerland)

(3) University of Salamanca, Facultad de Ciencias, Departamento de Geología, 37008, Salamanca (Spain)

Abstract

Recent coccoliths from 74 surface sediment samples recovered from the southeastern Pacific off Chile were examined quantitatively to investigate modern regional gradients of sea surface productivity and temperature. All findings are based on coccolith accumulations rates. Therefore an approach was designed to estimate recent sedimentation rates based on ^{210}Pb and bulk chemistry analyses of the same set of surface samples. Highest total coccolith accumulation rates were found off north-central Chile, where seasonal upwelling takes place. Based on a multiple linear regression between calculated coccolith accumulation rates and World Ocean Atlas derived sea surface temperatures, a calibration model to reconstruct annual average temperatures of the uppermost 75 m of the water column is provided. The model was cross-validated and the SST estimates were compared with SST observed and SST estimates based on diatoms and planktic foraminifera, showing a good correlation.

1. Introduction

Coccolithophores, one of the main open ocean primary producers, have a broad fossil record, which makes them an outstanding biostratigraphical group and gives them potential for paleontological study of ecosystem response to global change. As a basic requisite for their application as paleoceanographic proxies it is necessary to maximize the retrieval of paleoecological information from coccolithophore species, and to enhance the understanding of their ecology as a plankton group. Knowing how the present-day environment influences their spatial and temporal distribution, we could use the fossil record of such organisms to reconstruct the state and variation of past environments (Kucera et al., 2005).

One of the modern ocean's most productive upwelling conditions occur all along the Chilean margin (Strub et al., 1998; Abrantes et al., 2007). In coastal upwelling domains, the dominant primary producers are diatoms, although coccolithophores are also significant contributors to the total phytoplankton community (e.g., Mitchell−Innes and Winter, 1987; Giraudeau et al., 2000; Boeckel and Baumann, 2004). However, there are very few modern studies on coccolithophores ecology and calibration to climate proxies in the Southeast (SE) Pacific, and most of them are based on plankton samples (e.g., Beaufort et al., 2007; Beaufort et al., 2008; Beaufort et al., 2011) or on sediment trap samples (e.g., González et al., 2004; Köbrich, 2008). So far, only a small number of surface sediment studies were performed by Saavedra-Pellitero et al. (i.e., 2010; 2011). In such studies the ecological optima of the most important species of coccolithophores in the Pacific sector was studied in order to produced feasible transfer functions to reconstruct climate changes in the past. In this work the focus was on coccolithophore surface sediment assemblages since they represent the former living communities and with that, the overlying surface water conditions (Andruleit et al., 2004). While relative abundances indicate dominance of a certain ecological habitat, absolute fluxes represent more realistic living conditions in the water column, thus providing a more detailed reconstruction of hydrography (Ravelo et al., 1990). Coccolith accumulation rate (CAR) data could furthermore complement and in some cases improve upon the relative abundance data, whereas also comparing with modern flux estimates derived from sediment trap studies.

The estimation of past environmental parameters using micropaleontological data has became a very useful tool from the development of statistical transfer function techniques (IKM - Imbrie and Kipp Method) in which the authors originally used planktonic foraminifera (Imbrie and Kipp, 1971; Klovan and Imbrie, 1971). It provides quantitative estimations of hydrographical parameters (e.g., sea surface temperature, SST) preserved in the recent sedimentary record (e.g., CLIMAP 1976, 1981, Ortiz and Mix 1997, Pisias et al., 1997; Mix et al., 1999; Kucera et al., 2005; Morey et al., 2005; Abrantes et al., 2007). Different statistical techniques were already applied to coccolith census counts from surface sediments of the North and Equatorial Pacific (Geitzenauer et al., 1977; Roth and Coulbourn, 1982; Roth, 1994), of the North Atlantic (Geitzenauer et al., 1977) as well as of the Benguela upwelling system (Giraudeau and Rogers, 1994). However the different sample coverage, the different taxonomies (of traditional broad species) as well as the exclusion of species in some of those investigations prevented any transfer function to be properly defined. Consequently, a well established calibration of modern coccolithophore assemblages to surface mixed-layer temperatures has only been previously achieved at a few locations. These were performed at the Benguela and the Peru-Chile upwelling systems (Giraudeau and Rogers, 1994; Saavedra-Pellitero et al., 2010; 2011) and differ from ours by being based on species relative abundances. The main goal of the present study was to investigate whether the modern regional gradients of sea surface productivity and temperature can be detected by studying (a) coccolith accumulation rates and (b) coccolithophore derived temperature estimates.

1.1. Regional setting

The SE Pacific is dominated by the Peru-Chile current system (Strub et al., 1998), one of the most productive eastern boundary systems in the world. Off southern Chile, cool waters from the Antarctic Circumpolar Current reach the continent and split in two branches, the southward-flowing Cape Horn Current and the northward-flowing Peru Current (Fig. 1A). Coastal upwelling, driven by persistent southerly winds along the coast brings cold and nutrient-rich waters to the sea surface along the coast of Chile and Peru towards the equator (Wyrtki, 1981; Bryden and Brady, 1985; Strub et al., 1998). Phytoplankton biomass is high throughout the year in this coastal upwelling system (Rojas de Mendiola, 1981). However, from 15°S to 30°S, minimum chlorophyll seasonality offshore Chile is observed, despite strong seasonality in wind forcing between 20°S and 30°S. South of this area, chlorophyll reaches maxima during austral summer and minima in austral winter, in phase with the seasonal wind forcing (Thomas et al., 2004).

Precipitation patterns in Chile, the most important climate factor driving continental erosion, show one of the most pronounced latitudinal gradients on Earth (Kaiser, 2005; Hebbeln et al., 2007). Rainfall rates rapidly increases from almost zero in the hyper-arid Atacama desert (north of 27°S) over intermediate precipitation in the semi-arid Mediterranean-type climate of central Chile (from 31°S to 37°S) to year round humid conditions with extraordinary high annual precipitation south of 42°S (Miller, 1976; New et al., 2002). Major atmospheric circulation patterns, specifically the SE Pacific anticyclone in the north and the rain-bearing Southern Westerlies in the south, are responsible for this marked N-S gradient along Chile (Hebbeln et al., 2007, see Fig. 1B). However, expected differences in mass accumulation rates along the Chilean continental margin depend not only on the different hydrological regimes, but also on the topography of margin and on the latitudinal variability of primary productivity and upwelling (Muñoz et al., 2004).

2. Material and Methods

For this study we considered 74 out of 106 surface sediment samples located from 22.80ºS to 44.28ºS and from 70.49ºW to 75.86ºW offshore Chile. Previous studies (Saavedra-Pellitero et al., 2010; 2011) allowed us to select the best preserved samples and to exclude the samples where coccoliths were poorly preserved. The uppermost centimetre from the undisturbed surface sediment samples (boxcores and multicores), has been used for the analyses reported here. They were retrieved during Genesis III Cruise, RR9702A onboard the American R/V Roger Revelle and during R/V SONNE Cruise SO-156 Valparaiso-Talcahuano (Hebbeln and cruise participants, 2001) onboard the German R/V Sonne.

2.1. Coccolith counts and estimations of CARs

Coccolith absolute abundance counts were already available from a previous study (Saavedra-Pellitero et al., 2010) although only relative abundances were published in that paper. Slides for coccolith counts were prepared using the standard settling methodology of Flores and Sierro (1997). Coccolith identification was done using a Leica DMRXE and a Nikon Eclipse 80i polarized microscopes at a magnification of X1000, occasionally X1250. In order to ensure statistical reliability a minimum of 400 coccoliths per sample were counted. This procedure allowed us to estimate the total number of coccoliths per gram of sediment for each of the coccolithophore species and species CARs. We followed the taxonomy established by Hine and Weaver (1998), Bown and Young (1998) and the internet site www.nannotax.org. Some additional considerations were also taken into account (i.e., the group of *Gephyrocapsa* <3µm defined by Flores et al., 1997). The formula used to calculate CARs is:

$$CAR = [(n \cdot R^2 \cdot V^2)/(r^2 \cdot g \cdot v)] \cdot DBD \cdot SR$$

where n is the number of coccoliths counted in a random light microscope scanned area; R is the radius of the Petri dish used; V is the volume of the water added to the dry sediment; r is the radius of the visual field used in the counting; g is the dry sediment weight; *v* is the volume of mixture withdrawn with the micropipette; *DBD* is the estimated dry density of the sediment, and *SR* is the linear sedimentation rate.

2.2. Sedimentation rate estimates and dry bulk densities

Sedimentation rates (SRs) and sediment dry bulk densities (DBD) are required to estimate CARs. However the lack of these measurements for the majority of the samples considered in this study led us to design an approach to estimate them. To calculate the SR along the Chilean continental margin, we considered the recent SR data based on ^{210}Pb (Muñoz et al., 2004; Fig. 2A) available from a subset of samples spanning across a broad range of sedimentation regimes which correspond to some of the samples studied here (Figs. 1B and 2, Table 1). Owing to the fact that the samples cover very distinct areas and stations are quite sparsely distributed, we normalized the number of coccoliths per gram of sediment instead of directly interpolating the SR data from Muñoz et al. (2004; see Fig. 2). This designed approach consists of comparing the bulk chemistry analyses done by inductively coupled plasma atomic emission spectrometry (ICP-MS, Stuut et al., 2007), with the SR based on ^{210}Pb (Muñoz et al., 2004) using multiple regression analysis. Mesh grids were created for Al, Fe, K, Mg, and Ti derived by ICP-MS measurements with Matlab™ and the values for the 17 stations indicated in Table 1 were used for the calibration.

Stepwise multiple regression is a systematic method for choosing predictors (or independent variables) of a particular dependent variable on the basis of statistical criteria (Howitt and Cramer, 2008). This procedure determines which independent variable is the best predictor, the second best predictor, etc. After regressing our independent or predictor variables (Al, Fe, K, Mg, and Ti ICP-MS values, in our case) against the dependent variable (SR, in our case) with Matlab™ software, we found out that only Ti is positively correlated to SR (R^2=0.61, Fig. 2B and supplementary material). This relationship reflects the recent sedimentation patterns on the Chilean continental slope. A lack of significant precipitation limits the denudation in the Atacama Desert (Stuut et al., 2007) restricting the sediment supply to the Chilean margin and therefore the high SRs and Ti contents offshore North Chile. On the contrary, humid conditions and stronger erosion in South Chile (Miller, 1976) favors the higher SR and Ti contents at the southermost surface sediment samples. The linear equation obtained allowed us to estimate SR from Ti measurements for the specific case of the study area.

$$SR=(0.1089\cdot Ti)-0.274$$

This formula provided a way to estimate SR for the surface sediment samples studied (Table 2, Fig. 3A) with a root mean squared error (RMSE) of 0.047 for the 64 samples where ICP-MS were performed, all of them GeoB samples. Concerning the 10 non-GeoB stations of the database (RR-), euclidean distances between each station and the GeoB stations were calculated and the smallest one was chosen. For the four samples located further offshore, different SR values were considered (Table 1).

To estimate sediment DBDs, the closest value from Muñoz et al. (2004) was chosen (Table 1 for original measurements and Table 2 for estimates), except for the four further offshore stations, where the same criteria as for SR was followed.

2.3. Oceanographic variables of the surface waters

The modern oceanographic properties chosen for this work are sea surface temperature (SST in °C, Locarnini et al., 2006), sea surface salinity (SSS in PSU, Antonov et al., 2006), nitrate (micromole/l), phosphate (micromole/l), silicate (micromole/l, all data from Garcia et al., 2006) and chlorophyll concentrations (microgram/l, Levitus, 1982; Conkright and Boyer, 2002) expressed as an annual average from 0 m to 75 m water depth. In addition, depth of the mixing layer (m) and primary productivity (mg C/m^2/day) were considered. All these parameters were obtained from the World Ocean Atlas 2005, from the World Ocean Atlas 2001 Data Sets, National Oceanographic Data Centre, Washington DC (see http://ingrid.ldgo.columbia.edu/SOURCES/.NOAA/.NODC), and from Ocean Productivity (http://www.science.oregonstate.edu/ocean.productivity/index.php).
Euclidean distances between each station and World Ocean Atlas database (1° grid) were calculated and the smallest one was chosen using Matlab™. All the contour maps were generated using Ocean Data View (ODV) software (Schlitzer, 2011). The main model was generated with R software (for further details see section 3.2) and ordination was performed using the Vegan package for R (Oksanen et al., 2006).

3. Results

3.1. Coccolith accumulation rates

Maximum numbers of $2.21 \cdot 10^9$ coccoliths/g and highest CARs of $6.9 \cdot 10^7$ coccoliths/cm^2/yr are reached at different locations in the northernmost stations while minimum numbers of $2.10 \cdot 10^6$ coccoliths/g and CARs of $9.2 \cdot 10^4$ coccoliths/cm^2/yr are reached offshore southern Chile (44.06ºS, 75.13ºW, Fig. 3B, C).

The 14 most common taxa or groups of coccoliths regarded in this study are *Calciosolenia* spp., *Calcidiscus leptoporus*, *Coccolithus pelagicus*, *Emiliania huxleyi*, *Florisphaera profunda*, *Gephyrocapsa muellerae*, *Gephyrocapsa oceanica*, *Helicosphaera carteri*, *Rhabdosphaera clavigera*, small *Gephyrocapsa* (*Gephyrocapsa* <3µm), *Syracosphaera* spp., *Umbellosphaera* spp., *Umbilicosphaera* spp. and *Oolithotus* spp. In the following we briefly describe the main features observed in the contour maps (Fig. 4) ranging from highest CARs average to lowest ones for each coccolithophore taxa. Small *Gephyrocaps*a is the most abundant group (average of $1.94 \cdot 10^6$ coccoliths/cm^2/yr) which reaches abundances of $1.69 \cdot 10^7$ coccoliths/cm^2/yr at 26°S, although high numbers are also recorded in other parts of the Chilean upwelling area (Fig. 4A). *C. leptoporus* shows an average CAR of $1.48 \cdot 10^6$ coccoliths/cm^2/yr. Maximum CARs of up to $1.5 \cdot 10^7$ coccoliths/cm^2/yr for this species are reached in the samples located in the north of the study area and decrease towards the South (Fig. 4B). An average of $1.3 \cdot 10^6$ coccoliths/cm^2/yr was estimated for *F. profunda* (Fig. 4C). CARs for this lower photic zone dweller fluctuates considerably, decreasing broadly southwards; maximum values are reached at 26°S ($1.08 \cdot 10^7$ coccoliths/cm^2) and minimum at the southernmost locations offshore Chile ($8.59 \cdot 10^3$ coccoliths/cm^2/yr). *E. huxleyi*, with an average of $1.21 \cdot 10^6$ coccoliths/cm^2/yr, diplays a similar distribution pattern to small *Gephyrocaps*a with maximum CAR of $8.81 \cdot 10^6$ coccoliths/cm^2 (Fig. 4D).

G. muellerae occurs in average CARs of $1.10 \cdot 10^6$ coccoliths/cm^2/yr. This species fluctuates along the Chilean upwelling region; it reaches a maximum of $7.42 \cdot 10^6$ coccoliths/cm^2/yr in the northern part of the study area and high CARs at the southernmost locations (Fig. 4E). *G. oceanica*, with an average of $1.08 \cdot 10^6$ coccoliths/cm^2/yr, reaches maximum CARs ($9.74 \cdot 10^6$ coccoliths/cm^2/yr) at the northern part of the study area and progressively decreases southwards (Fig. 4F).

H. carteri shows average CARs of $5.24 \cdot 10^5$ coccoliths/cm^2/yr. Maximum CARs of this species are clearly reached in central and north offshore Chile ($6.19 \cdot 10^6$ coccoliths/cm^2/yr, Fig. 4G). *C. pelagicus* reaches average CARs of $9.73 \cdot 10^4$ coccoliths/cm^2/yr and its maxima ($7.19 \cdot 10^5$ coccoliths/cm^2/yr) at the southernmost locations of the Chilean upwelling (Fig. 4H). *Umbellosphaera* spp. shows average CARs of $8.86 \cdot 10^3$ coccoliths/cm^2/yr with maximum of $2.47 \cdot 10^5$ coccoliths/cm^2/yr (Fig. 4I).

Results corresponding to the rest of the coccolithophore species are not listed here either owing to their low numbers or to the non-relevance for the SST estimates. This refers to *Syracosphaera* spp. (average of $3.67 \cdot 10^4$ coccoliths/cm^2/yr), *Oolithotus* spp. (average of $1.98 \cdot 10^4$ coccoliths/cm^2/yr), *Umbilicosphaera* spp. (average of $1.06 \cdot 10^5$ coccoliths/cm^2/yr), *R. clavigera* (average of $5.19 \cdot 10^3$ coccoliths/cm^2/yr) and *Calciosolenia* spp. (average of $4.18 \cdot 10^3$ coccoliths/cm^2/yr).

3.2. Statistical analysis and SST transfer function

A preliminary detrended correspondence analysis (DCA) on the coccolithophore assemblage resulted in a gradient shorter than 2 Standard Deviation (SD) units, suggesting a linear response (ter Braak, 1987). Then, principal component analysis (PCA) was used to analyze the relationship between coccolithophore assemblage and environmental properties, where the latter variables have been entered passively, and to identify outlying samples with unusual assemblages (ter, Braak, 1987). There were no unusual samples, as indicated by the PCA. The significance of PCA axes was assessed using the broken-stick model, resulting in just one significant axis explaining 78.9% of the variance, and being highly correlated with SST. These results are in agreement with Saavedra-Pellitero (2011) who found out that SST was the dominant oceanographic parameter controlling certain coccolithophore species (grouped into a factor) offshore Chile. CARs were square transformed to standardize their variances. Rare species were downweighted because the square root transformation increases their weight and they can have undue influence on the ordination. To establish a SST-sensitive transfer function based on CAR, we performed a multiple linear regression. The number of parameters in the fitted model were determined using a Akaike's information criterion. Thus, the species eventually included in the minimal adequate model were: *F. profunda* (F.pro), *H. carteri* (H.car), *G. muellerae* (G.mue), *Umbellosphaera* spp. (Umbe) and *C. pelagicus* (C.pel). The minimal adequate regression and final calibration model showed a residual standard error of 0.803 on 66 degrees of freedom and adjusted R^2 of 0.7021. We obtained the following equation to estimate SST using CARs:

$$SST=12.98+[0.0015557\bullet(F.pro) + 0.0011031\bullet(H.car) -0.0009193\bullet(G.mue) - 0.0032570\bullet(Umbe)-0.0024363\bullet(C.pel)]$$

A root mean squared error of prediction (RMSEP) was assessed by (bootstrapping and jackknifing) cross-validation (99 permutation cycles) in order to assess the predictive power of our transfer function (Table 3). The final model was examined for potential outliers, because these can strongly affect transfer function coefficients and may markedly decrease the predictive ability of the model. Outliers were identified as samples having an absolute residual (observed minus estimated) higher than the SD of the environmental variable of interest and a low influence on the model indicated by Cook's D (Cook's D <4/n, Fig 5D). Based on this criterion, the samples GeoB 7108 and RR 52 mc3 were excluded.

The SST residuals (the difference between the observed minus the estimated SST) were tested for homoscedasticity (constant variance). This condition ensures that the best-fitting line works well for all relevant values of SST estimated, not just in certain areas. In the scatter plot of the standardized residuals against the SST estimated values (Fig. 5C) the spread in the residuals stays almost the same throughout, addressing the homoscedasticity condition. In general, the SST residuals are relatively low (most of them are between -1 and 1) and without any significant correlation or trend with the estimated SSTs (Fig. 5A). Our results based on CARs reveal good reproducibility of the SST World Ocean Atlas 2005 (see Fig. 6 and supplementary material). Even though we regarded annual averages to avoid any influence of seasonality, seasonal changes in oceanographic conditions can strongly influence the coccolithophore fluxes. Therefore SST residuals were also compared with the SST difference between summer and winter in the study area (Fig. 7A). A slight trend can be observed between SST difference and SST residuals (Fig. 7B)

4. Discussion

4.1. CARs estimates

Coccolith distribution patterns and coccolith numbers from surface sediment samples are dependent on coccolithophore productivity, on dissolution and on dilution by terrigenous material, which influences sedimentation rates. Due to the enormous differences in mass accumulation rates along the Chilean continental margin, CARs compliment and in some cases improve the relative data to reconstruct gradients in coccolithophore productivity off Chile. Highest total CARs are found in the stations located off north-central Chilean coast (22.8ºS-30ºS, Fig. 3), where seasonal upwelling takes place (18ºS-27ºS; Strub et al., 1998) and where Abrantes et al. (2007) observed samples barren of diatoms. However, a marked decrease in CARs is observed further offshore at surface sediment samples around ~23ºS (Fig. 3C). At these locations high numbers of coccoliths per gram of sediment are noted (Fig. 3B), yet CARs notably decrease with respect to more coastal samples at similar latitude, probably driven by low SRs estimates. High coccolithophore diversity is also recorded off north-central Chilean continental margin, as displayed by the presence of different placolith bearing species (i.e., small *Gephyrocapsa*, *C. leptoporus*, *E. huxleyi*, *G. muellerae* and *G. oceanica*) together with other coccolith forms (e.g., *F. profunda*, *H. carteri* and *Umbellosphaera* spp.). Offshore central-south Chile, upwelling-favorable conditions occur from late spring to early fall, corresponding to the most persistent upwelling extending from 35ºS to 38ºS (Strub et al., 1998). Due to the fact that underneath these high productive zones degradational processes of organic matter may favor enhanced carbonate dissolution (Boeckel and Baumann, 2004), samples barren of coccolithophores or highly affected by dissolution (which were excluded in our model) are mainly located in areas from 35.5°S to 39°S (Saavedra-Pellitero et al., 2010). A drop in the total CARs and in all the species numbers are observed in the area from 36.5ºS to 38ºS (Fig. 3) nearby the persistent upwelling cell off point Concepción (Strub et al., 1998) coincident with the highest diatom abundance values (valves/g) and organic carbon recorded in the same region by Abrantes et al. (2007). The only coccoliths recorded in this area (around ~36ºS) belong to *F. profunda* and *G. oceanica*, and in a lesser extent *E. huxleyi*, small *Gephyrocapsa*. and *G. muellerae*. The tongue of low-salinity water characteristic from the fjord region off south Chile (e.g., Lamy et al., 2002) has been recognized by maxima in the abundance of freshwater diatoms (Abrantes et al., 2007) and by the factors derived from the coccolith percentage dataset (Saavedra-Pellitero et al., 2010), but is not clearly defined by the CARs. The most prominent coccolithophore species in this area are *C. pelagicus* and *G. muellerae*, but small placoliths, such as small *Gephyrocapsa* and *E. huxleyi* are also present.

A comparison of the observed CARs with the coccolith flux collected from a sediment trap located offshore Chile (30°S, 73°11'W, Fig. 4) showed that numbers differ, although they are still comparable. A total CAR of $6.8 \cdot 10^6$ coccoliths/cm^2/yr, was obtained for the closest surface sediment sample in our dataset (29.72°S, 72.17°W), a minimum flux of $9.86 \cdot 10^6$ coccoliths/cm^2/yr was estimated during El Niño conditions (1997-1998) and an average of $1.59 \cdot 10^8$ coccoliths/cm^2/yr during non-El Niño conditions (1993-1994; Köbrich, 2008); at least the calculated CAR is in the order of the minimum flux during El Niño conditions. Owing to the fact that the surface sediment sample was not retrieved directly underneath the mooring location and that dissolution processes are likely to affect primarily deep sediments, differences between the CAR estimates and the sediment trap fluxes appear to be reasonable. In addition, the sediment trap recorded seasonal and annual variations while the surface sediment samples provided averaged data on a wider time interval of tens to hundreds of years.

4.2. Reliability of the SST reconstruction

The present SST estimation is adding to a series of previously published transfer functions in the SE Pacific realm based on data from different siliceous and calcareous microfossils, with the innovation of using species CARs from surface sediment samples instead of relative abundances. The results of our SST transfer function based on CARs reveal good reproducibility of the SST World Ocean Atlas 2005 (Locarnini et al., 2006) data; the estimated and measured SST values are highly correlated (R^2=0.723, Fig. 8B). We improved the spatial resolution offshore Chile, especially compared with previous works based on radiolarian census (Pisias et al., 1997; Pisias et al., 2006) and planktonic foraminifera (Mix et al., 1999; Feldberg and Mix, 2002; Kucera et al., 2005; Morey et al., 2005) which considered very few samples for the whole study area (see Fig. 8A). Abrantes et al. (2007) added some samples to previously collected databases (e.g., Schuette and Schrader, 1979; Romero and Hebbeln, 2003) and successfully obtained a SST diatom transfer function based directly on species percentages. Many of those samples were also used by Saavedra-Pellitero et al. (2011) to estimate SST using multivariate statistical analyses performed on modern coccolithophore census data from 15°N to 50.6°S and from 71°W to 93°W. With our work we covered an existing gap in the north-central Chilean coast (from ~23ºS to ~33ºS) due to the lack of preserved diatoms in the samples (Fig. 8A).

A comparison of the SST estimates derived from our model (using CARs) with previous SST transfer functions based on planktonic foraminifera (Kucera et al., 2005) and diatoms (Abrantes et al., 2007) was performed and they resulted in close agreement (Fig. 8A). Nevertheless, even if the three reconstructions follow the same trend, our SST estimates are always lower than the other two because we considered an annual SST average from 0 m to 75 m water depth, instead of 0 m (chosen for diatoms) or 10 m (chosen for planktonic foraminifera) SST annual averages. Those differences are indeed higher offshore north-central Chile and become smaller offshore central-south Chile, specifically at intense upwelling areas (e.g., around 36ºS, Fig. 8A). The underestimation of SST further offshore Chile around ~23ºS (Figs. 6C and 8A) would be linked to the calculation of SR at those locations. A SST average (from 0 m to 75 m) was considered due to the fact that coccolithophore production can also happen at deeper depths (e.g., *F. profunda*); this choice also allowed us directly to compare with the SST estimates based on coccolith percentages (Saavedra-Pellitero et al., 2011). Both reconstructions based on coccolithophores follow the same trend as the SST observed, although the SST CAR estimates fits better (see Fig. 8A), especially from ~26ºS to ~36ºS. In any case, it should be noted that SST estimates using different coccolith datasets and statistical approaches offshore Chile resulted in close agreement, as shown by the high correlation (R^2=0.71) between the SST coccolith percentage estimates and the SST CAR estimates (supplementary material).

Focusing more on the CAR transfer function, it can be noted that negative SST residuals indicate that the model overestimated the mean annual SST while positive residuals indicate that the model estimates underestimated this parameter. Although SST residuals calculated here are low, the contour map of SST residuals (Fig. 6C) shows that our model tends to underestimate SSTs at the northernmost locations and overestimate SSTs at the southernmost ones together with those stations from the area between ~34.5ºS and ~36.5ºS which are under the influence of the persistent upwelling region described by Strub et al. (1998). Abrantes et al. (2007) also got SST overestimates and SST underestimates at the northern- and southernmost locations of our study area, but not offshore central Chile. This can be just explained by the ecological dominance of diatoms over coccolithophores and/or by coccolith carbonate preservation which could affect coccolithophore species composition in the upwelling region near Concepción (from 35ºS to 38ºS). The slight trend observed between SST summer-winter difference and SST residuals (Fig. 7B) suggest that samples with SST underestimates (high positive residuals) are more affected by seasonality than samples with SST overestimates (low negative residuals). Therefore seasonality has, to some extent, an influence on the warm-water and cold-water coccolithophore taxa preserved in the surface sediment samples. Even considering the limitations of our regional approach, both the total and species CAR estimates give a general idea of the number of coccoliths/cm^2/yr preserved in the surface sediments offshore Chile, an upwelling region mainly dominated by diatoms, and furthermore allowed us to obtain an accurate SST reconstruction.

5. Conclusions

In this study the modern regional gradients of sea surface productivity and temperature offshore Chile were detected by studying (a) coccolith accumulation rates (CARs) and (b) coccolithophore derived sea surface temperature (SST) estimates. The main findings are as follows:

(1) CARs, calculated by using estimated sedimentation rates based on recent ^{210}Pb and bulk chemistry analyses of surface samples from the Chilean margin, clearly reveal that the accumulation of coccolithophores shows a strong statistical relationship to SST. Rigorous numerical methods have been used to quantify the inherent error of the model and to asses the reliability of the quantitative reconstruction for the average temperatures of the uppermost 75 m of the water column.

(2) Total CARs and species CARs reflect the regional upwelling conditions along the Chilean continental margin. Highest total CARs were found off north-central Chile, where seasonal upwelling occurs.

(3) There are five key coccolithophore species which as show by our model record SST information; these are *Florisphaera profunda*, *Helicosphaera carteri*, *Gephyrocapsa muellerae*, *Umbellosphaera* spp. and *Coccolithus pelagicus*.

(4) Differences between observed and estimated SST coincide with a persistent upwelling region between ~34.5ºS and ~36.5ºS, yielding warmer temperatures than expected.

(5) In short, our results demonstrate the good reconstructive skill of observed SSTs and are in close agreement to a series of previously published SST transfer functions in the Southeast Pacific realm based on species percentages from different siliceous and calcareous microfossils.

Acknowledgements

The authors are indebted to A. Cortina for his helpful ideas and suggestions. Sediments samples were kindly provided by D. Hebbeln, M. Mohtadi, O. Romero, A. Mix and F. Abrantes. We are also grateful to P. Muñoz and S. Nuñez Ricardo for the sediment dry bulk density unpublished data provided, and to J. Collins and W. Brocas for their assistance. Analyses and visualizations used for this paper were produced with the Giovanni online data system, developed and maintained by the NASA GES DISC.

This work was funded by the Spanish "Programa Nacional de Movilidad de Recursos Humanos del Plan Nacional de I+D+i" and specifically by the MEC Postdoc grant (EX2009-0177) awarded to Mariem Saavedra-Pellitero.

References

Abrantes, F., Lopes, C., Mix, A., Pisias, N., 2007. Diatoms in Southeast Pacific surface sediments reflect environmental properties. Quaternary Science Reviews 26, 155-169. doi: 10.1016/j.quascirev.2006.02.022..

Andruleit, H., Rogalla, U., Stäger, S., 2004. From Living Communities to Fossil Assemblages: Origin and Fate of Coccolithophores in the Northern Arabian Sea. Micropaleontology 50, 5-21.

Antonov, J.I., Locarnini, R.A., Boyer, T.P., Mishonov, A.V., Garcia, H.E., 2006. World Ocean Atlas 2005, in: Levitus, S. (Ed.), NOAA Atlas NESDIS 61. U.S. Government Printing Office, Washington, D.C.

Beaufort, L., Couapel, M., Buchet, N., Claustre, H., 2007. Calcite production by Coccolithophores in the South East Pacific Ocean: from desert to jungle. Biogeosciences 4, 3267-3299.

Beaufort, L., Couapel, M., Buchet, N., Claustre, H., Goyet, C., 2008. Calcite production by coccolithophores in the south east Pacific Ocean. Biogeosciences 5, 1101-1117.

Beaufort, L., Probert, I., de Garidel-Thoron, T., Bendif, E.M., Ruiz-Pino, D., Metzl, N., Goyet, C., Buchet, N., Coupel, P., Grelaud, M., Rost, B., Rickaby, R.E.M., de Vargas, C., 2011. Sensitivity of coccolithophores to carbonate chemistry and ocean acidification. Nature 476, 80-83. doi: 10.1038/nature10295.

Beck, C., Grieser, J., Rudolf, B., 2005. A New Monthly Precipitation Climatology for the Global Land Areas for the Period 1951 to 2000. DWD, Klimastatusbericht KSB 2004, ISSN 1437-7691, ISSN 1616-5063 (Internet), ISBN 3-88148-402-7, 181-190.

Boeckel, B., Baumann, K.H., 2004. Distribution of coccoliths in surface sediments of the south-eastern South Atlantic Ocean: ecology, preservation and carbonate contribution. Marine Micropaleontology 51, 301-320. doi: 10.1016/j.marmicro.2004.01.001.

Bown, P., Young, J.R., 1998. Introduction, in: Bown, P. (Ed.), Calcareous nannofossil biostratigraphy. Chapman and Hall, London, pp. 1-15.

Bryden, H.L., Brady, E.C., 1985. Diagnostic model of the three-dimensional circulation in the upper equatorial Pacific Ocean. Journal of Physical Oceanography 15, 1255-1273.

CLIMAP, Climate: Long-Range Investigation, Mapping, and Prediction Project Members, 1976. The surface of the Ice Age Earth. Science, 191, 1131-1137.

CLIMAP, Climate: Long-Range Investigation, Mapping, and Prediction Project Members, 1981. Seasonal reconstructions of the Earth’s surface at the Last Glacial Maximum. Geological Society of American Map Chart Series MC, 36, 1-18.

Conkright, M.E., Boyer, T.P., 2002. World Ocean Atlas 2001: Objective Analyses, Data Statistics, and Figures, in: Silver Spring, M. (Ed.), CD-ROM Documentation. National Oceanographic Data Center, Washington, D.C.

Feldberg, M.J., Mix, A.C., 2002. Sea-surface temperature estimates in the Southeast Pacific based on planktonic foraminiferal species; modern calibration and Last Glacial Maximum. Marine Micropaleontology 44, 1-29. doi: 10.1016/S0377-8398(01)00035-4.

Flores, J.A., Sierro, F.J., 1997. Revised technique for calculation of calcareous nannofossil accumulation rates. Micropaleontology 43, 321-324.

Flores, J.A., Sierro, F.J., Francés, G., Vázquez, A., Zamarreño, I., 1997. The last 100,000 years in the western Mediterranean: sea surface water and frontal dynamics as revealed by coccolithophores. Marine Micropaleontology 29, 351-366. doi: 10.1016/S0377-8398(96)00029-1.

Garcia, H.E., Locarnini, R.A., Boyer, T.P., Antonov, J.I., 2006. World Ocean Atlas 2005, in: Levitus, S. (Ed.), NOAA Atlas NESDIS 61. U.S. Government Printing Office, Washington, D.C.

Geitzenauer, K.R., Roche, M.B., McIntyre, A., 1977. Coccolith biogeography from North Atlantic and Pacific surface sediments; a comparison of species distribution and abundances, in: Ramsay, A.T.S. (Ed.), Oceanic Micropaleontology. Academic Press, London, pp. 973-1008.

Giraudeau, J., Rogers, J., 1994. Phytoplankton biomass and sea-surface temperature estimates from sea-bed distribution of nannofossils and planktonic foraminifera in the Benguela upwelling system. Micropaleontology 40, 275-285.

Giraudeau, J., Bailey, G.W., Pujol C., 2000. A high−resolution time−series analyses of particle fluxes in the northern Benguela coastal upwelling system: Carbonate record of changes in biogenic production and particle transfer processes. Deep Sea Research, Part II 47, 1999–2028. doi:10.1016/S0967-0645(00)00014-X.

González, H.E., Hebbeln, D., Iriarte, J.L., Marchant, M., 2004. Downward fluxes of faecal material and microplankton at 2300m depth in the oceanic area off Coquimbo (30°S), Chile, during 1993-1995. Deep Sea Research Part II: Topical Studies in Oceanography 51, 2457-2474. doi: 10.1016/j.dsr2.2004.07.027.

Hebbeln, D., Lamy, F., Mohtadi, M., Echtler, H., 2007. Tracing the impact of glacial-interglacial climate variability on erosion of the southern Andes. Geology 35, 131-134. doi: 10.1130/g23243a.1.

Hebbeln, D., Klump, J., Lamy, F., 2004.Sedimentology and geochemistry of core GIK17748-2. doi:10.1594/PANGAEA.226943.

Hebbeln, D. and cruise participants, 2001. PUCK: Report and preliminary results of R/V Sonne Cruise SO 156, Valparaiso (Chile)-Talcahuano (Chile), March 29-May 14, 2001. Berichte, Fachbereich Geowissenschaften, Universität Bremen, 182.

Hine, N., Weaver, P.P.E., 1998. Quaternary, in: Bown, P.R. (Ed.), Calcareous nannofossil biostratigraphy. Chapman & Hall, London, pp. 265-278.

Ho, S. L., Mollenhauer, G., Lamy, F., Martínez-Garcia, A., Mohtadi, M. , Gersonde, R., Hebbeln, D., Nuñez Ricardo, S., Rosell-Melé, A., Tiedemann, R., 2012. Sea surface temperature variability in the Pacific sector of the Southern Ocean over the past 700 kyr. Paleoceanography 27, PA4202. doi:10.1029/2012PA002317.

Howitt, D., Cramer, D., 2008. Introduction to SPSS in Psychology for version 16 and earlier 4th edition ed. Pearson/Prentice Hall, Harlow, England.

Imbrie, J., Kipp, N.G., 1971. A new micropaleontological method for Quantitative Paleoclimatology: Application to a late Pleistocene Caribbean Core, in: Turekian, K.K. (Ed.), The Late Cenozoic Glacial Ages. Yale University Press, New Haven, Connecticut, pp. 71-181.

Kaiser, J., 2005. Sea-surface temperature variability in the Southeast Pacific during the last Glacial-Interglacial cycle and Relationships to Paleoenvironmental changes in Central and Southern Chile, Fachbereich Geowissenschaften. Universität Bremen, Bremen.

Klovan, J.E., Imbrie, J., 1971. An algorithm and FORTRAN-IV program for large scale Q-mode factor analysis and calculation of factor scores. Mathematical Geology. 3, 61-77.

Klump, J., Hebbeln, D., Lamy, F., 2004. Sedimentology and geochemistry of core GeoB3302-1. doi:10.1594/PANGAEA.226935.

Köbrich, M.I.I., 2008. Seasonal dynamics and characterization of coccolithophore export production in two major upwelling regions. Cape Blanc (NW-Africa) & Chile (30°S), Fachbereich Geowissenschaften. Universität Bremen, Bremen..

Kucera, M., Weinelt, M., Kiefer, T., Pflaumann, U., Hayes, A., Weinelt, M., Chen, M.-T., Mix, A.C., Barrows, T.T., Cortijo, E., Duprat, J., Juggins, S., Waelbroeck, C., 2005. Reconstruction of sea-surface temperatures from assemblages of planktonic foraminifera: multi-technique approach based on geographically constrained calibration data sets and its application to glacial Atlantic and Pacific Oceans. Quaternary Science Reviews 24, 951-998. doi: 10.1016/j.quascirev.2004.07.014.

Lamy, F., Kaiser, J., 2009. Glacial to Holocene Paleoceanographic and Continental Paleoclimate Reconstructions Based on ODP Site 1233/GeoB 3313 Off Southern Chile, Past Climate Variability in South America and Surrounding Regions, pp. 129-156.

Lamy, F., Rühlemann, C., Hebbeln, D., Wefer, G., 2002. High- and low-latitude climate control on the position of the southern Peru-Chile Current during the Holocene. Paleoceanography 17. doi:10.1029/2001PA000727.

Lamy, F. , Hebbeln, D. and Wefer, G. (1999) High resolution marine record of climatic change in mid-latitude Chile during the last 28,000 years based on terrigenous sediment parameters. Quaternary Research, 51 , pp. 83-93 .

Levitus, S.E., 1982. Climatological atlas of the world ocean, in: Office, U.S.G.P. (Ed.), NOAA Professional Paper, Washington D.C.

Locarnini, R.A., Mishonov, A.V., Antonov, J.I., Boyer, T.P., Garcia, H.E., 2006. World Ocean Atlas 2005, in: Levitus, S. (Ed.), NOAA Atlas NESDIS 61. U.S. Government Printing Office, Washington, D.C.

Mitchell−Innes, B.A., Winter, A. 1987. Coccolithophores: A major phytoplankton component in mature upwelled waters off the Cape Peninsula, South Africa in March, 1983. Marine Biology 95, 25-30. doi:10.1007/BF00447481.

Miller, A., 1976. The climate of Chile., in: Schwerdtfeger, W.E. (Ed.), Climates of Central and South America. Elsevier, Amsterdam, pp. 113-145.

Mix, A.C., Morey, A.E., Pisias, N.G., Hostetler, S.W., 1999. Foraminiferal Faunal Estimates of Paleotemperature: Circumventing the No-Analog Problem Yields Cool Ice Age Tropics. Paleoceanography 14, 350-359. doi:10.1029/1999PA900012

Morey, A.E., Mix, A.C., Pisias, N.G., 2005. Planktonic foraminiferal assemblages preserved in surface sediments correspond to multiple environment variables. Quaternary Science Reviews 24, 925-950. doi: 10.1016/j.quascirev.2003.09.011.

Muñoz, P., Lange, C.B., Gutiérrez, D., Hebbeln, D., Salamanca, M.A., Dezileau, L., Reyss, J.L., Benninger, L.K., 2004. Recent sedimentation and mass accumulation rates based on ^{210}Pb along the Peru–Chile continental margin. Deep Sea Research Part II: Topical Studies in Oceanography 51, 2523-2541.

New, M., Lister, D., Hulme, M., Makin, I., 2002. A high-resolution data set of surface climate over global land areas. Climate Research 21, 1-25.

Oksanen, J., Kindt, R., Legendre, P., O’Hara, R. B., 2006. Vegan: Community Ecology Package version 1.8-2. http://cran.r-project.org.

Ortiz, J. D., Mix, A. C., 1997. Comparison of Imbrie-Kipp transfer function and modern analog temperature estimates using sediment trap and core-top foraminiferal faunas, Paleoceanography 12, 2, 175-190.

Pisias, N.G., Heusser, L., Heusser, C., Hostetler, S.W., Mix, A.C., Weber, M., 2006. Radiolaria and pollen records from 0 to 50 ka at ODP Site 1233: continental and marine climate records from the Southeast Pacific. Quaternary Science Reviews 25, 455-473. doi: 10.1016/j.quascirev.2005.06.009.

Pisias, N.G., Roelofs, A., Weber, M., 1997. Radiolarian-Based Transfer Functions for Estimating Mean Surface Ocean Temperatures and Seasonal Range. Paleoceanography 12, 365-379. doi: 10.1029/97PA00582.

Ravelo, A.C., Fairbanks, R.G., Philander, S.G.H., 1990. Reconstructing Tropical Atlantic Hydrography Using Planktontic Foraminifera and an Ocean Model. Paleoceanography 5, 409-431. doi: 10.1029/PA005i003p00409.

Rojas de Mendiola, B., 1981. Seasonal phytoplankton distribution along the Peruvian Coast, in: Richards, F.A.E. (Ed.), Coastal Upwelling. Coastal Estuarine Studies. AGU, Washington, pp. 339-347.

Romero, O., Hebbeln, D., 2003. Biogenic silica and diatom thanatocoenosis in surface sediments below the Peru-Chile Current: controlling mechanisms and relationship with productivity of surface waters. Marine Micropaleontology 48, 71-90. doi: 10.1016/S0377-8398(02)00161-5.

Roth, P.H., 1994. Distribution of coccoliths in oceanic sediments, in: Winter, A., Siesser, W.G. (Eds.), Coccolithophores. Cambridge University Press, Cambridge, pp. 199-218.

Roth, P.H., Coulbourn, W.T., 1982. Floral and solution patterns of coccoliths in surface sediments of the North Pacific. Marine Micropaleontology 7, 1-52. doi: 10.1016/0377-8398(82)90014-7.

Saavedra-Pellitero, M., Flores, J.-A., Baumann, K.-H., Sierro, F.-J., 2010. Coccolith distribution patterns in surface sediments of Equatorial and Southeastern Pacific Ocean. Geobios 43, 131-149. doi: 10.1016/j.geobios.2009.09.004.

Saavedra-Pellitero, M., Flores, J.A., Lamy, F., Sierro, F.J., Cortina, A., 2011. Coccolithophore estimates of paleotemperature and paleoproductivity changes in the southeast Pacific over the past ~27 kyr. Paleoceanography 26, PA1201. doi: 10.1029/2009pa001824.

Schlitzer, R., 2011. Ocean Data View, http://odv.awi.de.

Schuette, G., Schrader, H., 1979. Diatom taphocoenoses in the coastal upwelling area off Western South America. Nova Hedwigia 64, 359-378.

Strub, P.T., Mesias, J.M., Montecino, V., Ruttlant, J., Salinas, S., 1998. Coastal ocean circulation off Western South America, in: Robinson, R., Brink, K.H. (Eds.), The Global Coastal Ocean. Regional Studies and Syntheses, Wiley, pp. 273-315.

Stuut, J.-B.W., Kasten, S., Lamy, F., Hebbeln, D., 2007. Sources and modes of terrigenous sediment input to the Chilean continental slope. Quaternary International 161, 67-76. doi: 10.1016/j.quaint.2006.10.041.

ter Braak, C. J. F, 1987. The analysis of vegetation-environment relationships by canonical correspondence analysis. Vegetatio 69, 69-77.

Thomas, A.C., Strub, P.T., Carr, M.E., Weatherbee, R., 2004. Comparisons of chlorophyll variability between the four major global eastern boundary currents.

International Journal of Remote Sensing 25, 1443-1447. doi: 10.1080/01431160310001592418.

Tomczak, M., Godfrey, J.S., 2003. Regional Oceanography: an Introduction. 2nd improved edition. Daya Publishing House, Delhi.

Wyrtki, K., 1981. An estimate of equatorial upwelling in the Pacific. Journal of Physical Oceanography 11, 1205-1214.

Figure Caption1

Figure. 1. A. Map of the Pacific and adjacent areas showing major surface currents (after Tomczak and Godfrey, 2003; modified from Lamy and Kaiser, 2009). The study area has been indicated with yellow rectangle.
B. Sea Surface Temperature (SST in °C, Locarnini et al., 2006) expressed as an annual average from 0 m to 75 m water depth and annual mean precipitation (mm/yr) over parts of South America in 2000 (Beck et al., 2005).
The location of the sampling stations offshore Chile corresponding to recent sedimentation (SR) data available based on ^{210}Pb (Muñoz et al., 2004) is indicated with blue crosses, the sampling stations corresponding to ICP-MS measurements (Stuut et al., 2007) with black dots, and the 74 sea surface sediment samples used in this study with red dots.

Figure1
Click here to download high resolution image

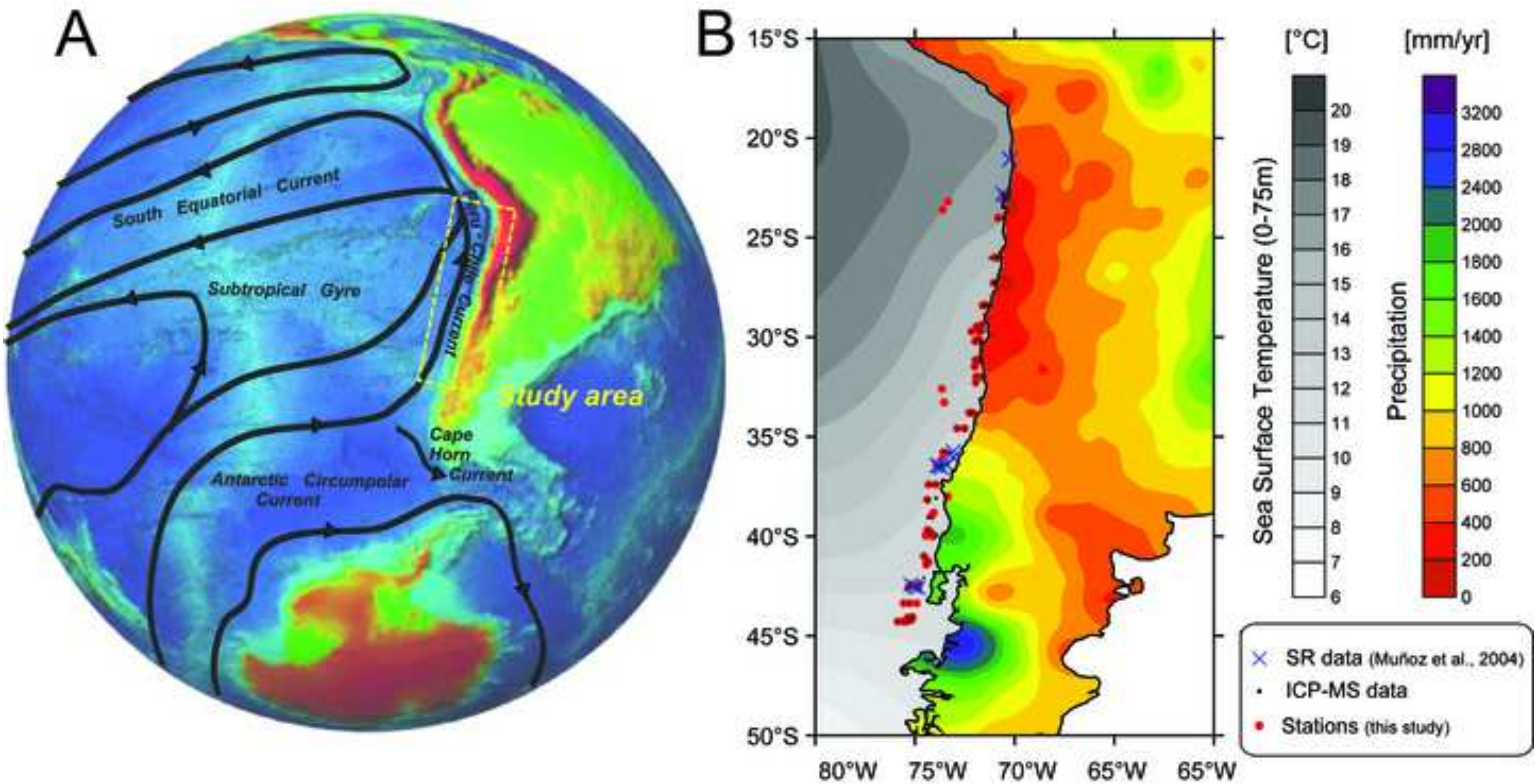

Figure Caption2

Figure 2. A. Sedimentation Rates (cm/yr) used in this work, from Muñoz et al. (2004), Lamy et al. (1999) and Ho et al. (2012).
B. Sedimentation Rates (cm/yr) from Muñoz et al. (2004) versus Ti (‰) values from the bulk chemistry analyses done by inductively coupled plasma atomic emission spectrometry (ICP-MS; Stuut et al. 2007).
C. Dry bulk densities (g/cm^3) used in this work, from Muñoz et al. (2004), Hebbeln et al. (2004), Klump et al. (2004), Muñoz and Nuñez pers. comm.

Figure 2
Click here to download high resolution image

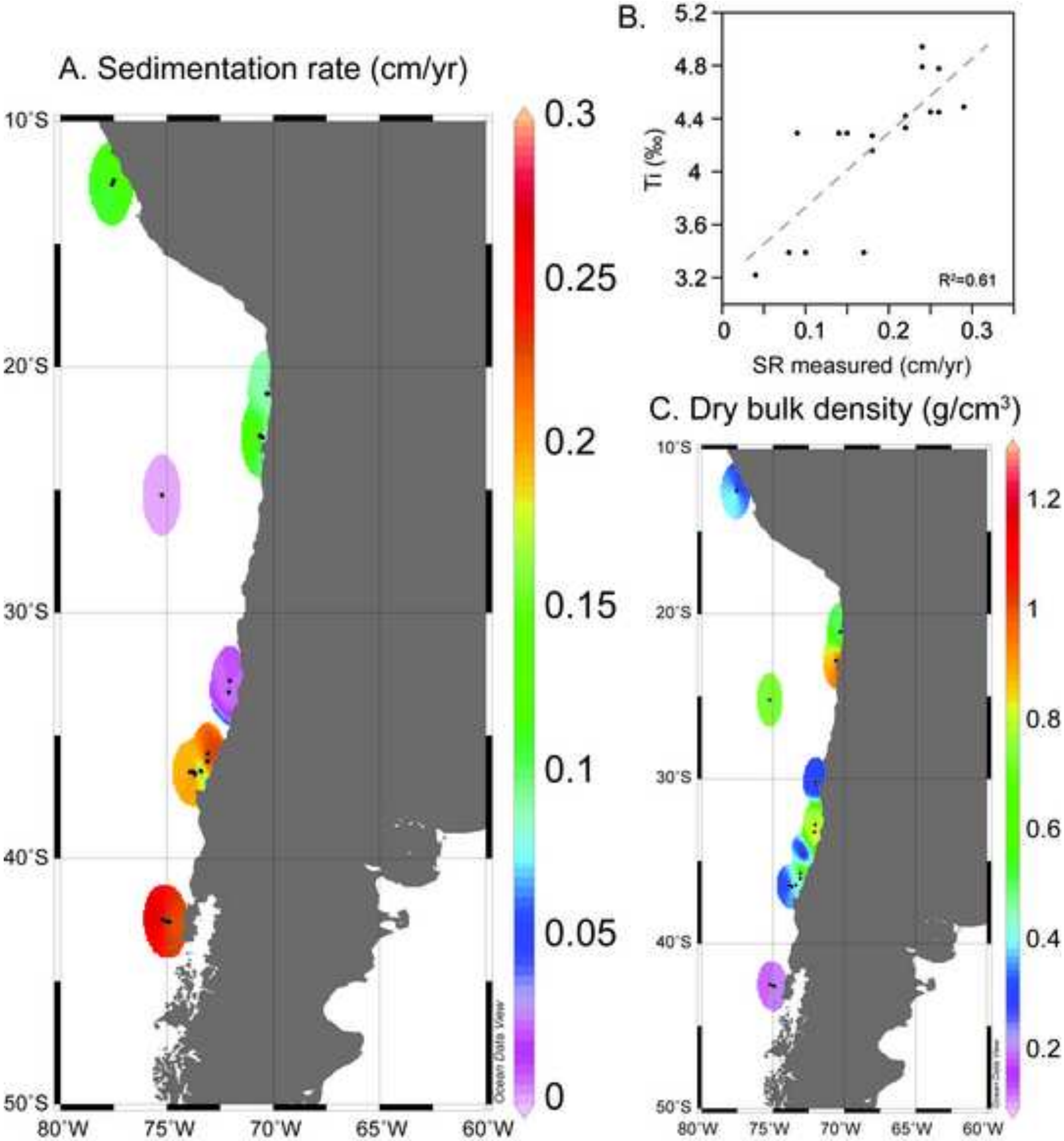

Figure Caption3

Figure 3. A. Sedimentation Rate estimates (cm/yr) for the study area using the present approach explained within the text. B. Total number of coccoliths per gram of sediment. C. Coccolith Accumulation Rate (CAR, coccoliths/cm^2/yr). The 74 surface sediment sample locations are indicated here with black dots.

Figure3
Click here to download high resolution image

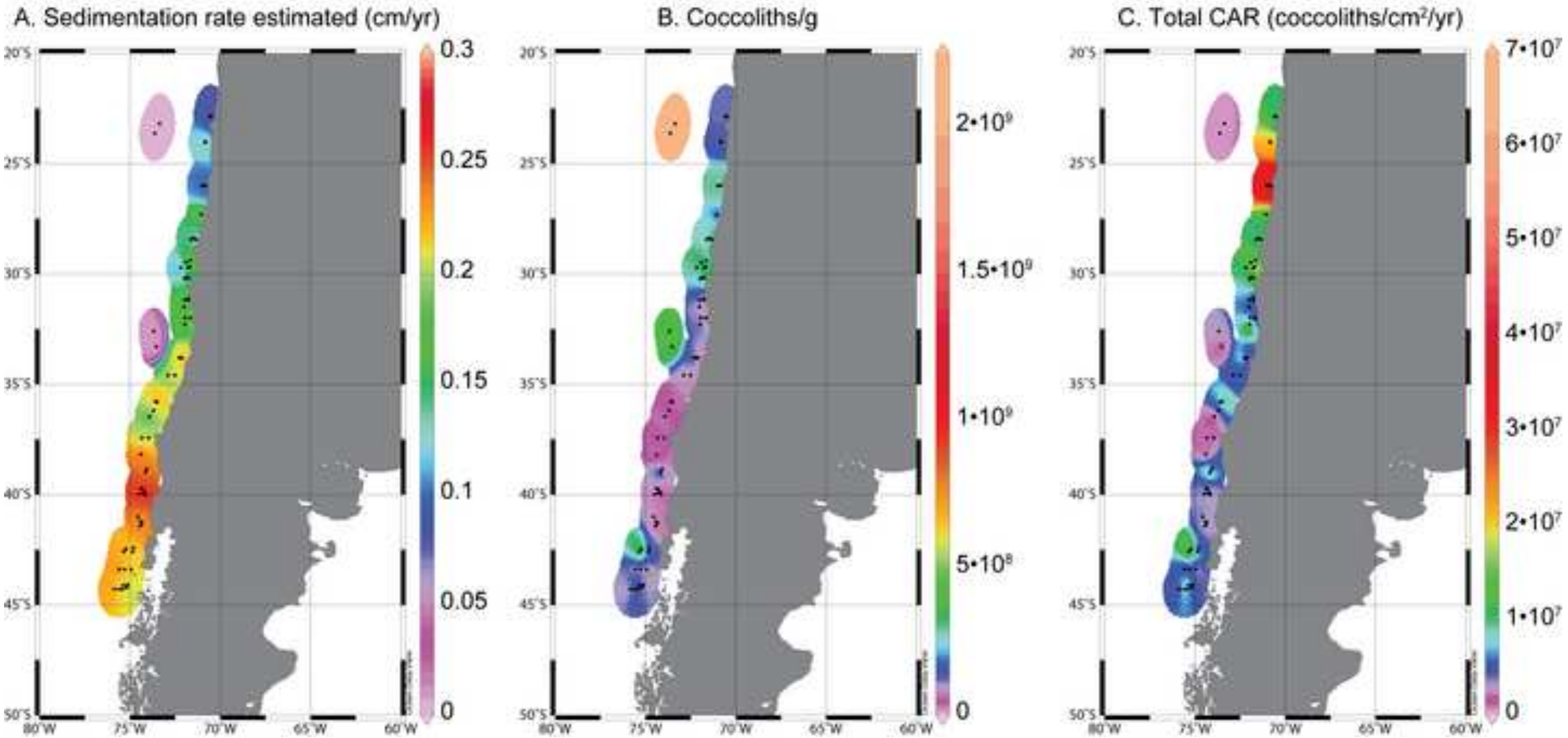

Figure Caption4

Figure 4. Distribution maps of Coccolith Accumulation Rates for the more important taxa or groups of coccoliths considered in the study area: A. “small” *Gephyrocapsa*, B. *Calcidiscus leptoporus, C. Florisphaera profunda*, D. *Emiliania huxleyi*, E. *Gephyrocapsa muellerae, F. Gephyrocapsa oceanica, G. Helicosphaera carteri, H. Coccolithus pelagicus* and I. *Umbellosphaera* spp. Stations are indicated with black dots. The gray star indicates the location of the sediment trap deployed off Chile (30°S, 73°11’W; González et al., 2004; Köbrich, 2008).

Figure4

Click here to download high resolution image

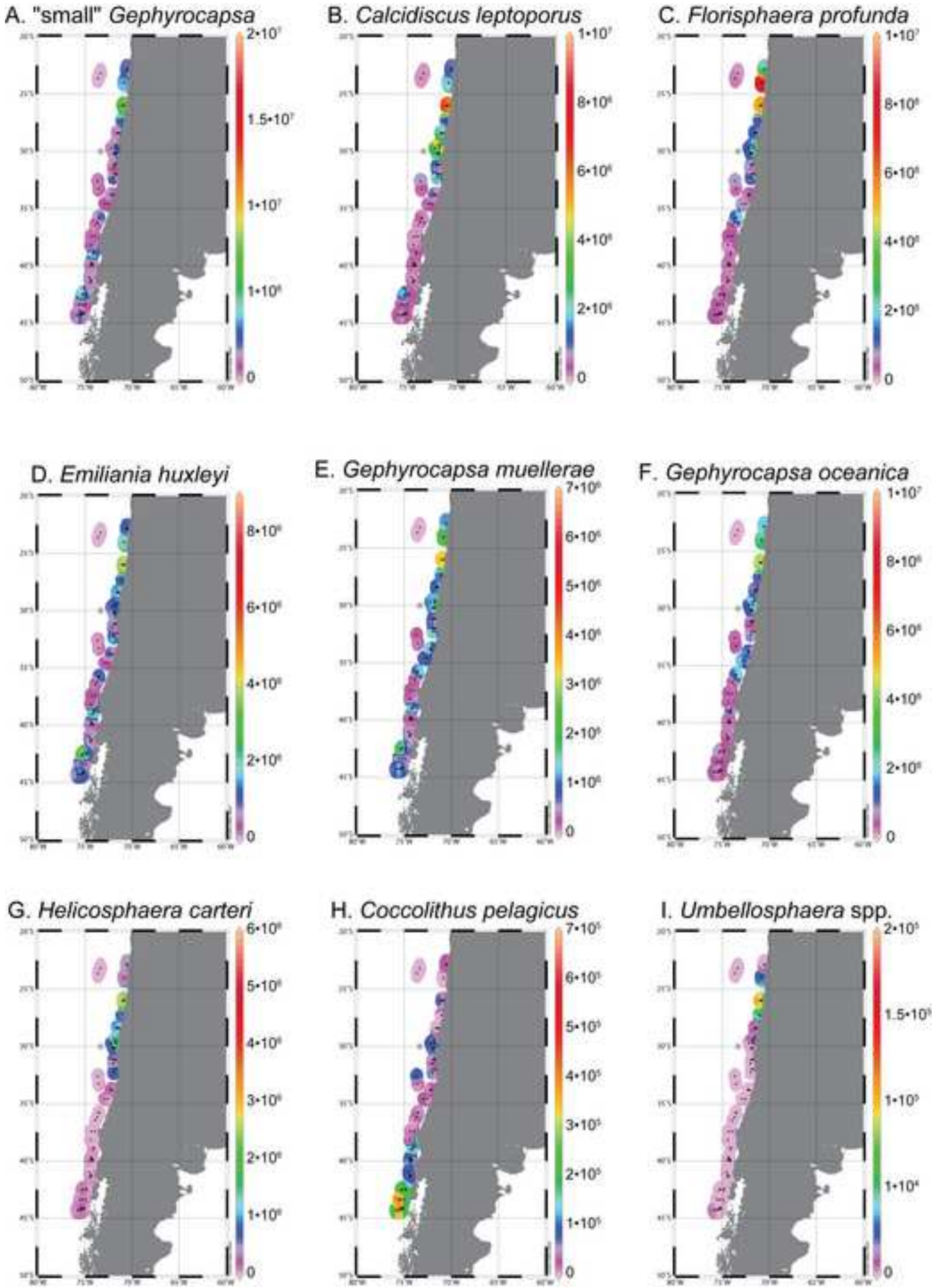

Figure Caption5

Figure 5. A. SST residuals versus SST estimated. B. Normal Q-Q. C. Scale location. D. SST residuals versus leverage.

Figure5

Click here to download high resolution image

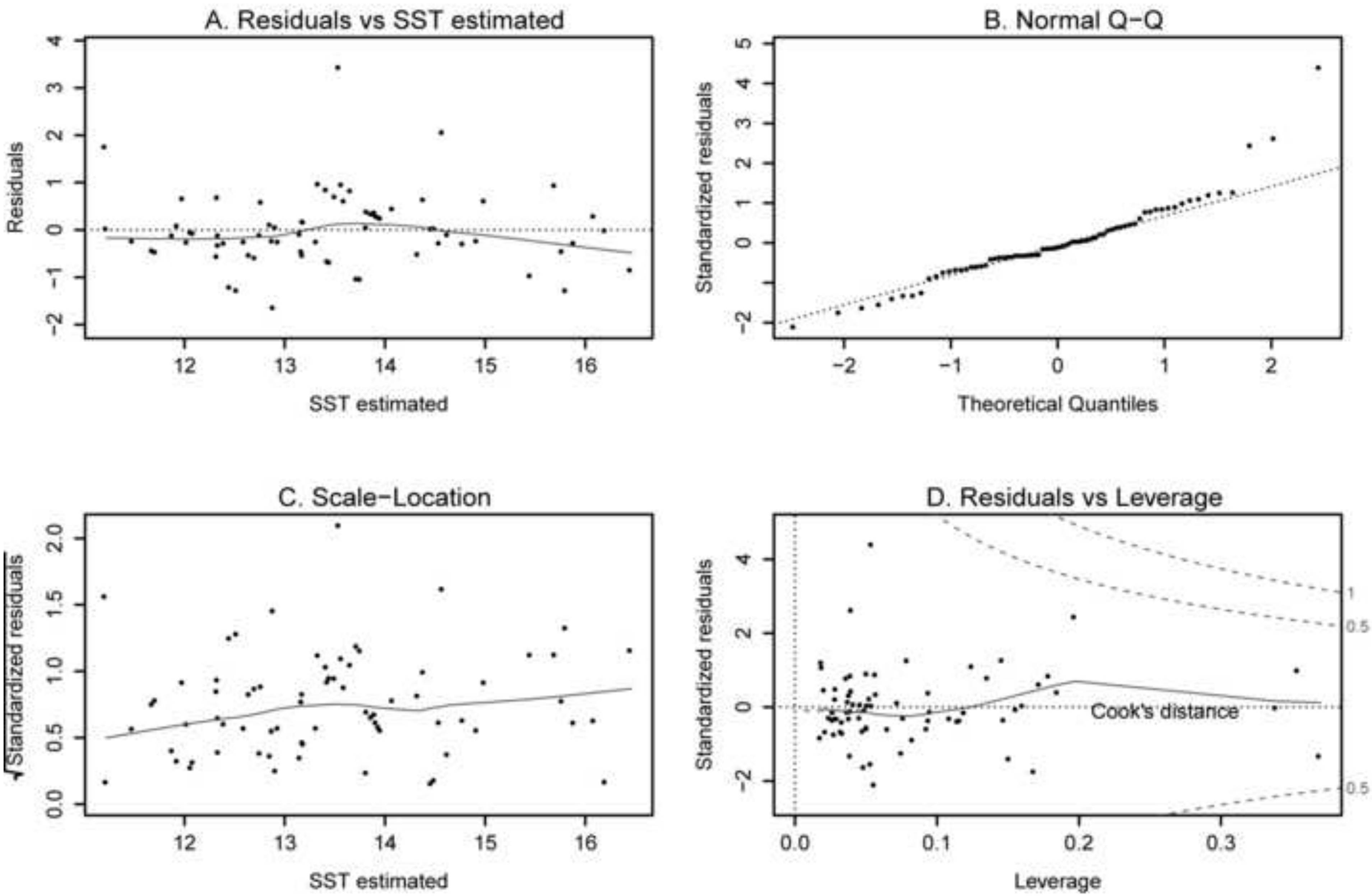

Figure Caption6

Figure 6. A. Annual 0-75 m SST average observed (in °C, from WOA05, Locarnini et al., 2006). B. Annual average 0-75 m SST estimated (in °C). C. Sea Surface Temperature residuals (SST estimated-SST observed). Stations are indicated with black dots.

Figure6
Click here to download high resolution image

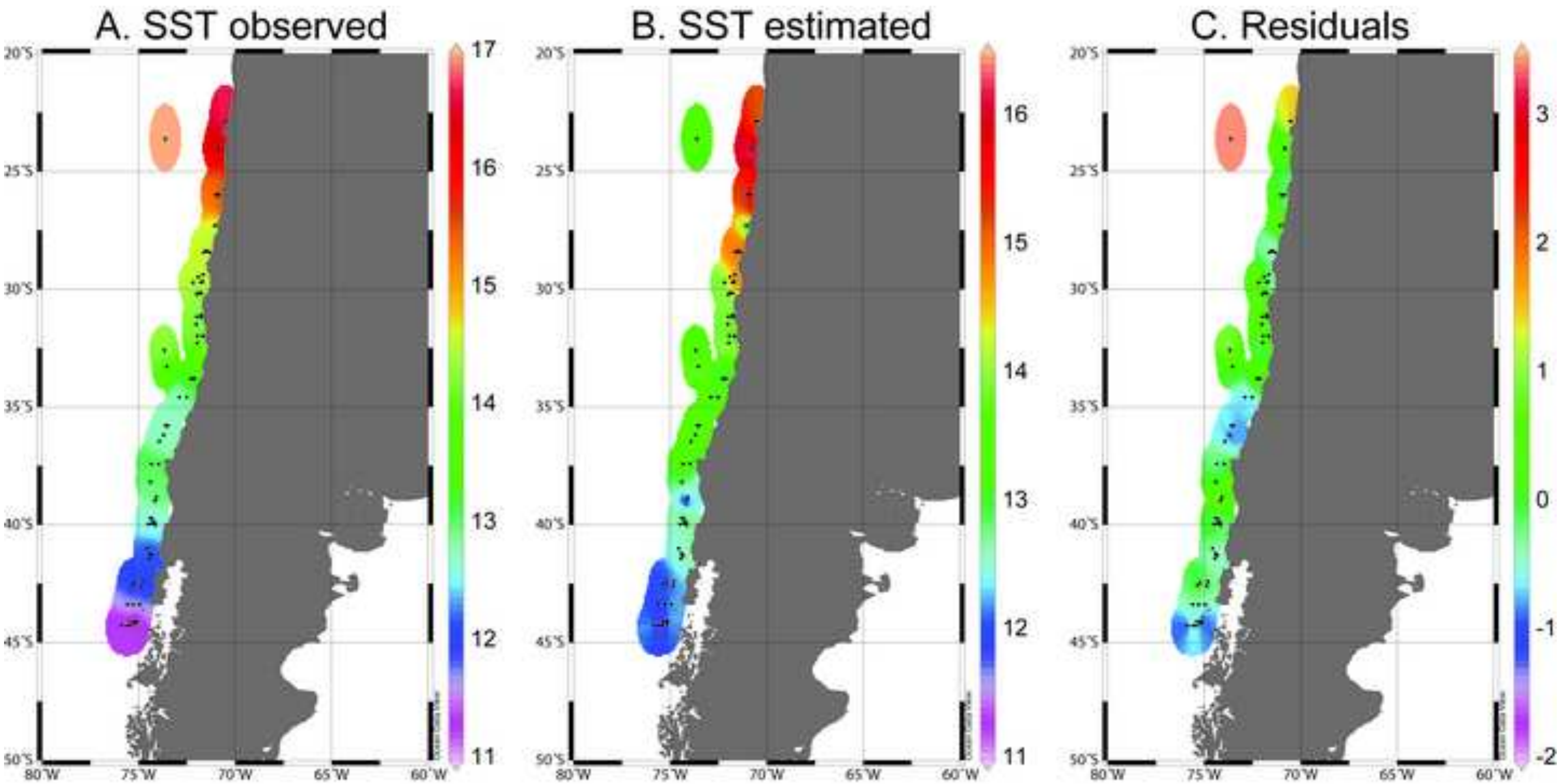

Figure Caption7

Figure 7. A. SST summer - SST winter (in °C). Data retrieved from WOA05 (Locarnini et al., 2006). The one-degree grid is indicated with black dots and stations with white dots. B. SST summer - SST winter versus SST residuals.

Figure7
Click here to download high resolution image

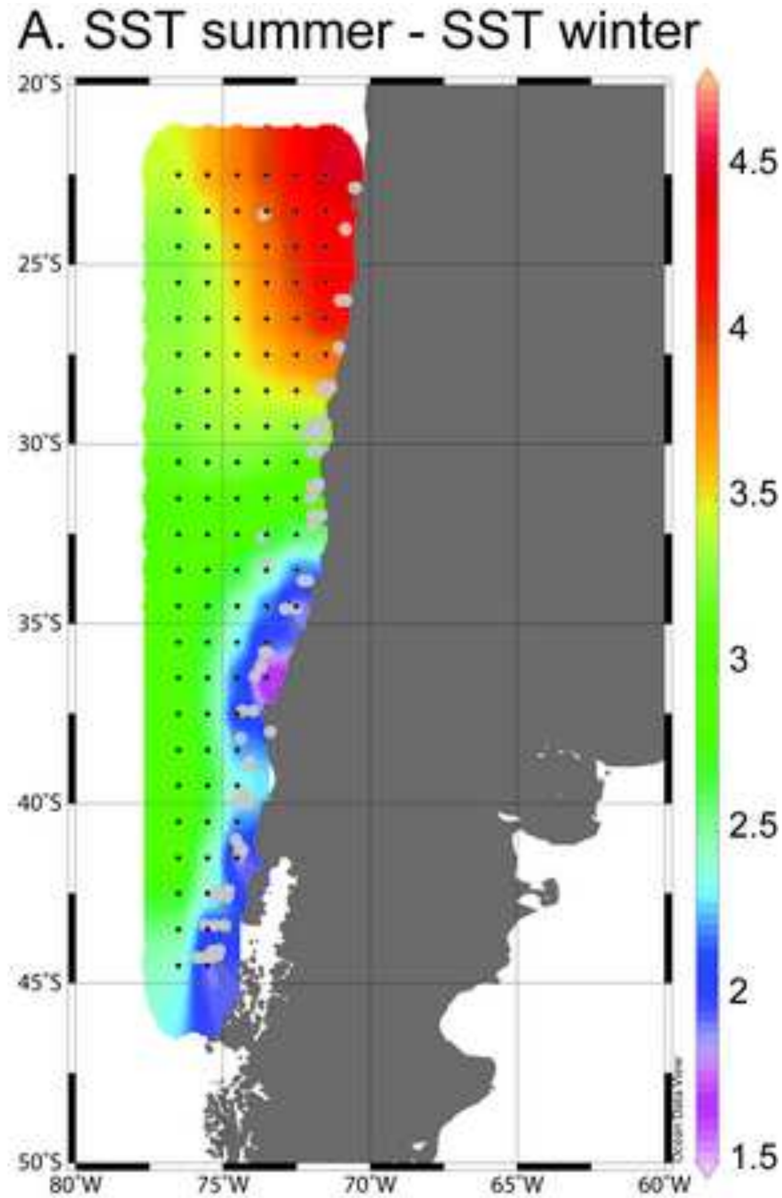

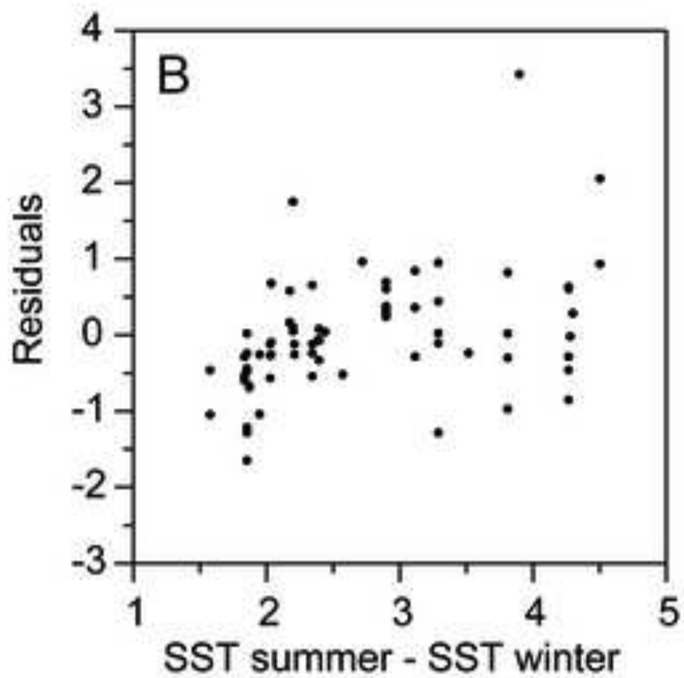

Figure 8. A. Sea Surface Temperature reconstruction (SST in °C, 0-75 m) using Coccolith Accumulation Rates (CARs) indicated with squares and pink line, SST observed (0-75 m, from WOA05, Locarnini et al., 2006) indicated with circles and orange line, SST reconstruction (0-75 m) using coccolithophore percentages (Saavedra-Pellitero et al., 2011) indicated with dashed line and green triangles, SST reconstruction with foraminifera at 10m (Kucera et al., 2005) indicated with blue squares with an asterisk inside and SST reconstruction with diatoms at 0 m depth (Abrantes et al., 2007). B. SST estimated versus SST observed (both in °C). The line represents the best fitting linear regression.

Figure8
Click here to download high resolution image

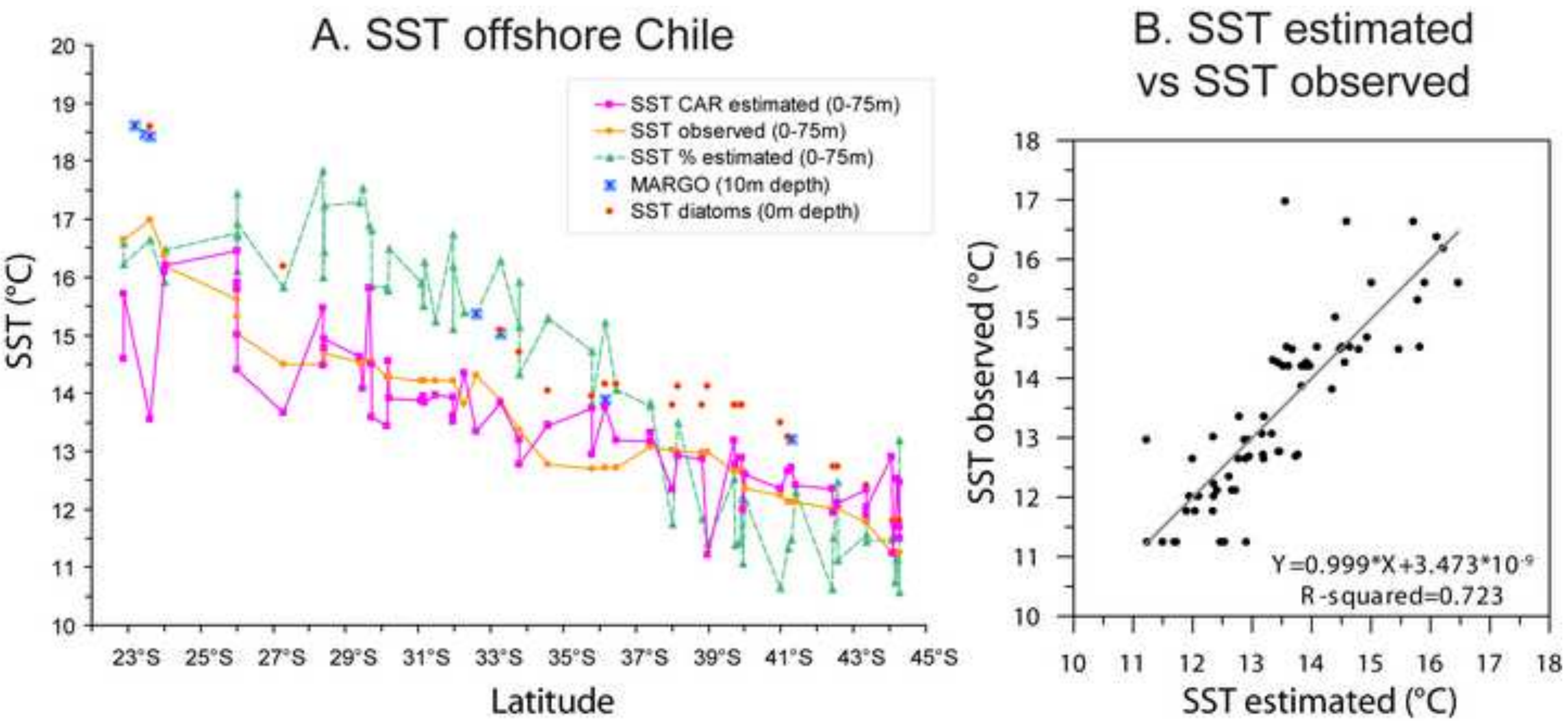

Table Captions

Table 1. Station, geographical position, measured sedimentation rate (SR, in cm/yr), authors of SR measurements, measurements of dry bulk density (DBD, in g/cm^3), authors of DBD measurements, Al, Fe, K, Mg and Ti (‰) values selected from the bulk chemistry analyses done by inductively coupled plasma atomic emission spectrometry (ICP-MS; Stuut et al. 2007). Underlined stations were used for the SR-Ti approach.

Table 2. List of studied samples including geographical position as well as estimated Sedimentation Rates (SR, in cm/yr), estimated Dry Bulk Densities (DBDs, in g/cm^3) and observed annual Sea Surface Temperature (SST in °C) average from 0 m to 75 m water depth (Locarnini et al., 2006). Asteriks indicate samples in which coccolithophore studies were not performed; for further details, see Saavedra-Pellitero et al. (2010). GeoB samples were retrieved during R/V SONNE Cruise SO-156 and RR samples during Genesis III Cruise RR9702A.

Table 3. Root mean squared error (RMSE), adjusted R^2, F-statistic, degrees of freedom and p-value of the 5 component model. Root mean squared error of prediction (RMSEP) of the model assessed by bootstrapping and jackknifing.

Table1

Click here to download Table: TABLE 1 table dry bulk densities and SR Measured.xls

Station	Longitude	Latitude	SR measured (cm/yr)		Author (SR)	DBD measured (g/cm3)	Author (DBD)	Al (‰)	Fe (‰)	K (‰)	Mg (‰)	Ti (‰)
Sta. A	-77.5	-12.4	0.13	±0.02	Muñoz et al., 2004	0.18	Muñoz et al., 2004					
Sta. C	-77.6	-12.6	0.1	±0.01	Muñoz et al., 2004	0.53	Muñoz et al., 2004					
Sta. 6	-70.2	-21.1	0.1	±0.01	Muñoz et al., 2004	0.45	Muñoz et al., 2004	48.11	60.36	19.70	17.01	3.390
Sta. 7	-70.3	-21.1	0.08	±0.01	Muñoz et al., 2004	0.54	Muñoz et al., 2004	48.11	60.36	19.70	17.01	3.390
GeoB 7104	-70.5	-22.9	0.04	±0.01	Muñoz et al., 2004	1.22	Muñoz et al., 2004	46.21	31.41	12.86	15.15	3.220
GeoB 7106	-70.6	-22.8	0.17	±0.003	Muñoz et al., 2004	0.67	Muñoz et al., 2004	48.11	60.36	19.70	17.01	3.390
5d	-73.1	-35.7	0.24	±0.05	Muñoz et al., 2004	0.75	Muñoz et al., 2004	83.39	43.47	14.08	13.96	4.943
4c	-73.1	-36.0	0.26	±0.03	Muñoz et al., 2004	0.44	Muñoz et al., 2004	80.86	41.90	13.29	14.55	4.778
GeoB 7160	-73.1	-36.0	0.24	±0.07	Muñoz et al., 2004	0.42	Muñoz et al., 2004	80.93	42.09	13.31	14.61	4.791
26A	-73.4	-36.4	0.09	±0.01	Muñoz et al., 2004	0.32	Muñoz et al., 2004	74.93	43.41	10.40	15.24	4.291
26B	-73.4	-36.4	0.14	±0.02	Muñoz et al., 2004	0.55	Muñoz et al., 2004	74.93	43.41	10.40	15.24	4.290
GeoB 7161	-73.4	-36.4	0.15	±0.01	Muñoz et al., 2004	0.30	Muñoz et al., 2004	74.93	43.41	10.40	15.24	4.290
3	-73.7	-36.5	0.26	±0.10	Muñoz et al., 2004	0.51	Muñoz et al., 2004	77.43	43.71	12.72	14.42	4.448
GeoB 7162	-73.7	-36.6	0.25	±0.04	Muñoz et al., 2004	0.31	Muñoz et al., 2004	77.44	43.67	12.68	14.43	4.450
GeoB 7166	-73.8	-36.5	0.18	±0.02	Muñoz et al., 2004	0.33	Muñoz et al., 2004	73.45	43.94	12.58	15.23	4.270
GeoB 7167	-73.9	-36.5	0.18	±0.02	Muñoz et al., 2004	0.23	Muñoz et al., 2004	72.10	42.56	12.40	15.86	4.159
GeoB 7177	-74.8	-42.6	0.22	±0.01	Muñoz et al., 2004	0.20	Muñoz et al., 2004	62.83	41.54	0.00	18.81	4.331
GeoB 7174	-75.0	-42.5	0.22	±0.02	Muñoz et al., 2004	0.23	Muñoz et al., 2004	64.60	41.96	0.00	18.36	4.421
GeoB 7175	-75.2	-42.5	0.29	±0.04	Muñoz et al., 2004	0.17	Muñoz et al., 2004	66.40	42.38	0.00	17.59	4.489
GeoB 7139	-72.0	-30.2	-			0.30	Muñoz, pers. comm.					
GeoB 7155	-72.9	-34.6	-			0.27	Muñoz, pers. comm.					
GIK 17748-2	-72.0	-32.8	0.009		Lamy et al., 1999	0.77	Hebbeln et al., 2004					
GIK 3302-1	-72.1	-33.2	0.006		Lamy et al., 1999	0.85	Klump et al., 2004					
GeoB 3388-1	-75.2	-25.2	0.0003		Ho et al., 2012	0.74	Nuñez Ricardo, pers comm.					

Table2

Click here to download Table: TABLE 2 SR calculated.xls

Station	Longitude	Latitude	Estimated SR	Estimated DBI	SST average (0-75 m)	Station	Longitude	Latitude	Estimated SR	Estimated DBI	SST average (0-75 m)
GeoB 7108	-70.6	-22.8	0.077	0.670	16.64	GeoB 7211	-74.3	-39.9	0.255	0.170	12.65
GeoB 7104	-70.5	-22.9	0.077	1.220	16.64	RR 20 mc4	-74.5	-40.0	0.255	0.170	12.65
GeoB 7103	-70.5	-22.9	0.077	1.220	16.64	RR 22 mc3	-74.1	-40.0	0.255	0.200	12.35
RR 52 mc3	-73.4	-23.2	0.0003	0.740	16.98	GeoB 7197	-74.6	-41.0	0.240	0.170	12.23
RR 50 mc2	-73.6	-23.6	0.0003	0.740	16.98	GeoB 7195	-74.4	-41.2	0.234	0.200	12.12
GeoB 7114	-70.8	-24.0	0.113	1.220	16.38	RR 24 mc3	-74.3	-41.3	0.234	0.200	12.12
GeoB 7112	-70.8	-24.0	0.148	1.220	16.19	GeoB 7194	-74.4	-41.4	0.234	0.200	12.12
GeoB 7118	-70.8	-26.0	0.100	1.220	15.61	GeoB 7172	-74.8	-42.4	0.227	0.200	12.02
GeoB 7122	-70.8	-26.0	0.100	1.220	15.61	GeoB 7175	-75.2	-42.5	0.215	0.170	12.02
GeoB 7119	-70.9	-26.0	0.100	1.220	15.32	GeoB 7179	-75.3	-42.6	0.229	0.170	12.02
GeoB 7121	-70.9	-26.0	0.100	1.220	15.61	GeoB 7177	-74.8	-42.6	0.197	0.200	12.02
GeoB 7116	-71.0	-26.0	0.100	1.220	15.03	GeoB 7182	-74.9	-43.4	0.212	0.200	11.77
GeoB 7123	-71.1	-27.3	0.196	0.300	14.49	GeoB 7181	-75.3	-43.4	0.212	0.230	11.77
GeoB 7127	-71.5	-28.4	0.158	0.300	14.49	GeoB 7180	-75.6	-43.4	0.242	0.170	11.77
GeoB 7131	-71.5	-28.4	0.145	0.300	14.49	GeoB 7183	-75.1	-44.1	0.218	0.200	11.25
GeoB 7129	-71.3	-28.4	0.103	0.300	14.49	GeoB 7192	-75.4	-44.1	0.217	0.230	11.25
GeoB 7130	-71.6	-28.4	0.138	0.300	14.69	GeoB 7186	-75.2	-44.2	0.197	0.200	11.25
GeoB 7133	-71.6	-29.4	0.213	0.300	14.53	GeoB 7187	-75.2	-44.2	0.194	0.200	11.25
GeoB 7132	-71.9	-29.5	0.142	0.300	14.53	GeoB 7189	-75.4	-44.3	0.216	0.230	11.25
GeoB 7135	-71.7	-29.7	0.164	0.300	14.53	GeoB 7191	-75.6	-44.3	0.209	0.230	11.25
GeoB 7134	-71.8	-29.7	0.143	0.300	14.53	GeoB 7190	-75.9	-44.3	0.232	0.230	11.25
GeoB 7136	-72.2	-29.7	0.082	0.300	14.53	GeoB 7115 (*)	-70.6	-24.0			
GeoB 7138	-71.9	-30.1	0.128	0.300	14.27	GeoB 7140 (*)	-71.8	-31.0			
GeoB 7137	-71.7	-30.2	0.172	0.300	14.27	RR 44 mc2 (*)	-73.0	-35.8			
GeoB 7139	-72.0	-30.2	0.115	0.300	14.27	GeoB 7159 (*)	-73.2	-35.8			
GeoB 7141	-71.8	-31.1	0.176	0.300	14.21	GeoB 7160 (*)	-73.1	-36.0			
GeoB 7144	-72.0	-31.2	0.176	0.300	14.21	RR 39 mc2 (*)	-73.6	-36.2			
GeoB 7142	-71.8	-31.2	0.176	0.300	14.21	GeoB 7161 (*)	-73.4	-36.4			
GeoB 7149	-72.0	-31.5	0.158	0.300	14.21	GeoB 7163 (*)	-73.6	-36.4			
GeoB 7146	-71.6	-32.0	0.202	0.300	14.21	GeoB 7166 (*)	-73.8	-36.5			
GeoB 7148	-71.9	-32.0	0.174	0.300	14.21	RR 34 mc5 (*)	-73.4	-36.5			
GeoB 7147	-71.7	-32.0	0.202	0.300	14.21	GeoB 7162 (*)	-73.7	-36.5			
GeoB 7150	-72.0	-32.3	0.157	0.770	13.82	GeoB 7170 (*)	-74.1	-37.4			
RR 48 mc4	-73.7	-32.6	0.009	0.770	14.31	RR 31 mc2 (*)	-75.4	-37.7			
RR 46 mc1	-73.5	-33.3	0.006	0.850	13.87	RR 29 mc2 (*)	-75.7	-37.8			
GeoB 7152	-72.1	-33.8	0.203	0.270	13.36	GeoB 7205 (*)	-73.7	-38.0			
GeoB 7153	-72.2	-33.8	0.234	0.270	13.36	GeoB 7204 (*)	-73.8	-38.0			
GeoB 7154	-72.3	-33.8	0.201	0.270	13.36	GeoB 7203 (*)	-74.0	-38.0			
GeoB 7156	-72.5	-34.6	0.207	0.270	12.77	GeoB 7201 (*)	-74.1	-38.1			
GeoB 7155	-72.9	-34.6	0.194	0.270	12.77	GeoB 7202 (*)	-73.9	-38.1			
GeoB 7158	-73.5	-35.8	0.219	0.750	12.69	GeoB 7200 (*)	-74.1	-38.2			
GeoB 7157	-73.6	-35.8	0.218	0.750	12.69	GeoB 7199 (*)	-74.3	-38.2			
RR 42 mc1	-73.7	-36.2	0.197	0.327	12.72	GeoB 7219 (*)	-73.6	-39.8			
GeoB 7167	-73.9	-36.5	0.179	0.227	12.72	RR 25 mc2 (*)	-75.9	-39.9			
GeoB 7171	-74.0	-37.4	0.202	0.313	13.07	GeoB 7218 (*)	-73.9	-39.9			
GeoB 7169	-74.3	-37.4	0.199	0.227	13.07	GeoB 7216 (*)	-73.9	-40.1			
GeoB 7207	-73.4	-38.0	0.220	0.313	13.02	RR 27 mc4 (*)	-75.9	-40.5			
GeoB 7198	-74.4	-38.2	0.239	0.313	12.97	GeoB 7173 (*)	-74.6	-42.1			
GeoB 7215	-74.1	-38.8	0.239	0.313	12.97	GeoB 7174 (*)	-75.0	-42.5			
GeoB 7209	-74.2	-39.0	0.239	0.313	12.97	RR 12 mc2 (*)	-76.3	-43.4			
GeoB 7212	-74.4	-39.7	0.255	0.170	12.65	RR 14 mc2 (*)	-76.5	-43.5			
GeoB 7213	-74.3	-39.7	0.255	0.170	12.65	RR 08 mc6 (*)	-76.7	-46.4			
GeoB 7214	-74.2	-39.9	0.255	0.170	12.65	RR 06 mc4 (*)	-76.6	-46.9			

Table3

Prediction model (5 components)	
RMSE	0.803
Adjusted R-squared	0.702
F-statistic	34.470
Degrees of freedom	66
p-value	< $2.2e^{-16}$
$RMSEP_{jacknifing}$	0.848
$RMSEP_{bootstrapping}$	0.869